Hindawi
Advances in Civil Engineering
Volume 2020, Article ID 1323296, 11 pages
https://doi.org/10.1155/2020/1323296

Research Article

Effect of Particle-Size Gradation on Coarse Sand-Geotextile Interface Response in Cyclic and Postcyclic Direct Shear Test

Jun Wang,[1] Meng-Jie Ying,[2] Fei-Yu Liu,[3] Hong-Tao Fu,[4] Jun-Feng Ni,[4] and Jing Shi[2]

[1]*Architecture and Civil Engineering College, Wenzhou University, Wenzhou 325025, Zhejiang, China*
[2]*Department of Civil Engineering, Shanghai University, Shanghai 200444, China*
[3]*College of Architecture and Civil Engineering, East China Jiaotong University, Nanchang 330013, China*
[4]*Department of Civil Engineering and Architecture, Saga University, Saga 840-8502, Japan*

Correspondence should be addressed to Fei-Yu Liu; lfyzju@shu.edu.cn

Received 28 February 2019; Revised 12 June 2019; Accepted 22 May 2020; Published 3 September 2020

Academic Editor: Castorina S. Vieira

In order to investigate the influence of sand particle-size gradation on cyclic and postcyclic shear strength behaviour on sand-geotextile interfaces, a series of monotonic direct shear (MDS), cyclic direct shear (CDS), and postcyclic direct shear (PCDS) tests were performed using a large-scale direct shear apparatus. The influence of cyclic shear history on the direct shear behaviour of the interface was studied. The results indicated that cyclic shear stress degradation occurred at the sand-geotextile interface. Shear volumetric contraction induced by the cyclic direct shear increased with the increase in cycle number. The lowest final contraction value was observed in discontinuously graded sand. In the MDS tests, there were great differences in interface shear strength due to the different particle-size gradations, whereas the differences between shear volumes were negligible. In the PCDS tests, the shear stress-displacement curves exhibited postpeak stress hardening behaviour for different particle-size gradations, and differences in shear volumes were detected. The well-graded sand-geotextile interface had a higher value of shear stiffness and a higher damping ratio relative to the other interfaces. Postcyclic shear stress degradation was observed for the discontinuously graded sand-geotextile interface.

1. Introduction

Soil reinforcement techniques were firstly put forward by Vidal [1] and have been widely applied in geotechnical engineering. The geotextile-reinforced soil structures, including reinforced retaining wall, slope, and embankment, play a vital role in the construction of infrastructure such as highway, railway, port, and airport. Recently, different laboratory experimental research studies and numerical simulations have been conducted on these structures [2–5].

Wang et al. [6, 7] revealed that soil-geotextile interaction plays a significant contribution in the stability and bearing capacity of earth structures. The ability of geotextile enhances the performance of retaining walls and embankment in terms of reducing the surface deformation. Further, the interaction mechanism between soil and geosynthetic needs to have a clear understanding and more accurate determination. So, various experimental studies have been made to investigate the interface mechanism by direct shear tests, pull-out tests, inclined plane tests, and torsional ring shear tests [8–11]. Among these testing methods, the direct shear method is one of the most commonly used methods in determining the frictional behaviour of geosynthetic-soil interface.

A series of factors may have significant impacts on the static shear behaviour of soil-geosynthetic interface. Afzali-Nejad et al. [12] investigated the influence of particle shape on shear strength and dilation of sand-woven geotextile interfaces. Infante et al. [13] showed that the interface shear strength was significantly affected by the factors of type of geosynthetics and density of soils. Ferreira et al. [14] examined the influences of soil moisture content and geosynthetic type on the soil-geosynthetic interface. Anubhav and Basudhar [15] concluded that the particle shape was an

important parameter to study the interface behaviour. It was found that the frictional behaviour of reinforced soil interface was mainly influenced by the properties of soil and properties of reinforcement.

Cyclic direct shear tests are performed to characterize the interaction near the base of the slope between two materials in reinforced soil structures under traffic, seismic, and other types of cyclic loading. Liu et al. and Wang et al. [2, 16] discussed the effect of soil particle size on the cyclic and postcyclic shear behaviour between sand and geogrid interface. Alaie and Chenari [17] conducted the monotonic, cyclic, and postcyclic tests in EPS-sand-geogrid mixtures. Under cyclic direct shear tests, there is also a need to understand the interlocking on sand-geotextile interface. The effect of particle-size gradation on cyclic shear strength has not been fully studied. Furthermore, the comparison between monotonic direct shear tests and postcyclic direct shear behaviour under the effect of particle-size gradation on cyclic shear tests requires further discussion and investigation.

The primary objective of this study is to investigate the effect of sand particle-size gradation on shear behaviours of the sand-geotextile interface via laboratory large-scale direct shear test. The sand used in the tests was classified based on the grain diameter. Both monotonic direct shear (MDS) and cyclic direct shear (CDS) tests were performed under different normal stresses. The interface shear properties, including shear stiffness, damping ratios, and shear strength envelope, were specifically examined in detail.

2. Materials and Methods

2.1. Testing Apparatus. The direct shear testing device used in this study is the ShearTrac-III Large-Scale Direct Shear Apparatus designed and constructed by Geocomp. The device consists of an upper box with dimensions of 305 mm × 305 mm in length and width and 100 mm in height and a lower box of 305 mm × 405 mm in length and width and 100 mm in height. The maximum horizontal displacement is 100 mm. The lower box is larger than the upper box, which ensures a constant contact area throughout the shearing process. The device can apply static shear as well as cyclic shear, and these effects can be either load-controlled or displacement-controlled. For this study, displacement-controlled tests were performed. The upper box is fixed in the horizontal direction, whereas the lower box moves horizontally, driven by high-accuracy electric motors. The maximum shearing rate is 15 mm/min. The loading system shows good control of the normal stress during testing, and even significant volumetric contraction is recorded by a liner variable differential transformer (LVDT), respectively.

2.2. Test Materials. The test materialwasselected as the coarse silica sand with a specific gravity (Gs) of 2.65. This coarse sand was divided into four classes by screening for grain size. The particle sizes (diameter) of the four classes were*S*1 (0.5–1 mm), *S*2 (1–2 mm), *S*3 (2–4 mm), and *S*4 (4–8 mm). According to the Unified Soil Classification System (USCS), these four classes of coarse sand were mixed in predetermined proportions and classified as well-graded coarse sand (*C*1), poorly graded coarse sand (*C*2), and discontinuously graded coarse sand (*C*3). The coefficient of uniformity (C_u) of three samples were 5.71, 3.23, and 1.72, and the coefficient of curvature (C_c) were 1.43, 0.81, and 0.87. The particle-size distribution curves of the sands are presented in Figure 1. The woven geotextile was used in this paper. The properties of the geotextile are listed in Table 1.

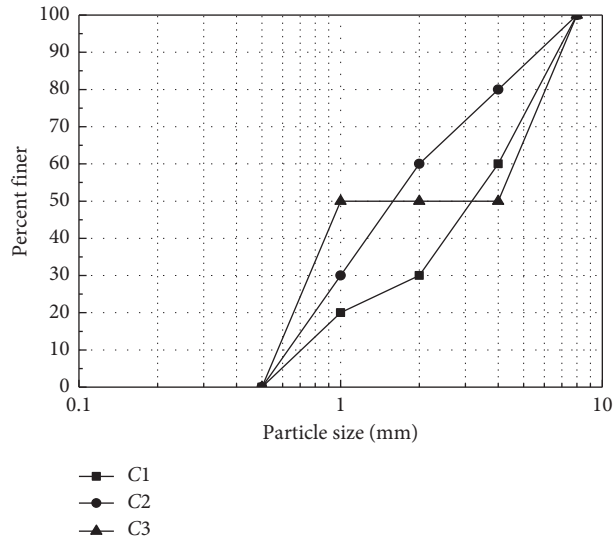

Figure 1: Particle-size distribution curves for the test sands.

2.3. Testing Procedures. A series of CDS, MDS, and PCDS tests were conducted to evaluate shear behaviours of the coarse sand-geotextile interfaces. According to ASTM D5321 [18], the shearing displacement rate was designated as 1 mm/min of 30, 60, and 90 kPa for all tests, the shear displacement amplitude for the CDS tests was designated as 3 mm, and the number of cycles was designated as 10. The top surface of the sand was kept as horizontal as possible until the specified elevation was reached, at which time the total mass of sand loaded was recorded. During each test, a rigid block was placed in the lower box. The geotextilewas fixed over the lower box with bolts and steel blocks to ensure that there was no relative displacement between the material and the lower box. The shear occurred along the sand-geotextile interface. The validity of the method of placing rigid blocks in the lower box has been demonstrated in [19]. The cyclic shear path is shown in Figure 2(a). The lower shear box moved from the equilibrium position following the shear path ①-②-③-④, which was defined as one loading cycle. After the CDS test was completed, the normal stress applied to the sample was unloaded and reloaded to the target value of the PCDS test. The MDS tests without cyclic shearing were performed on the reloaded specimens.

Table 1: Main characteristics of the geotextile.

Geotextile	Mass per unit area (g/m^2)	Trapezoidal tearing strength (kN/m)		Elongation at break (%)		Ultimate tensile strength (kN/m)	
		TD	LD	TD	LD	TD	LD
Woven geotextile	150	0.4	0.4	28	28	20	28

TD, transverse direction; LD, longitudinal direction.

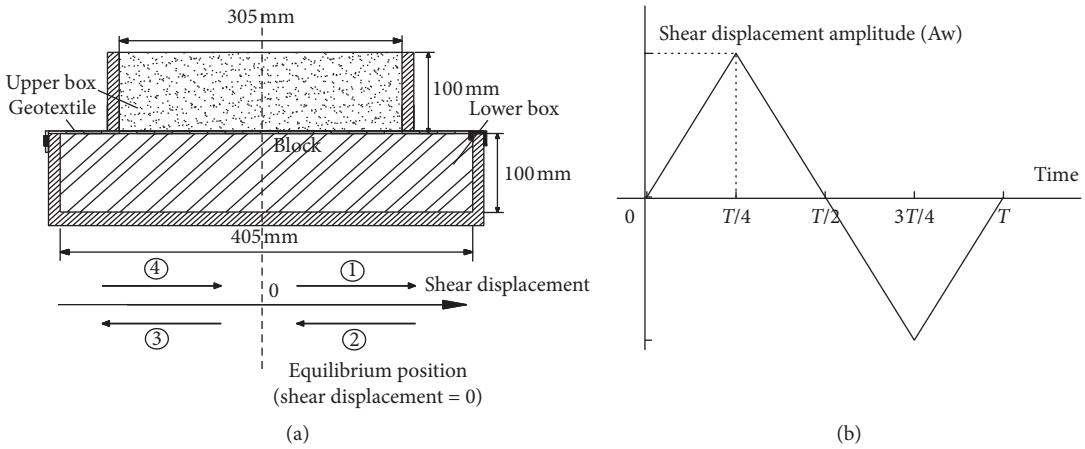

Figure 2: Schematic of the cyclic shear paths. (a) The cyclic shear path. (b) Waveform of cyclic load.

3. Cyclic Direct Shear Test Results

The shear stress versus shear displacement curves for the results of the CDS tests with the three interfaces under normal stress of 90 kPa are shown in Figure 3. The peak shear stress in the hysteresis loops decreases with increasing number of cycles, and the sand-geotextile interface shear strength tends to show cyclic shear softening for all three particle-size gradations. This phenomenon is mainly caused by interface wear and deformation, which changes the mechanical properties of the geotextile under cyclic shearing [20]. In each shear cycle, the peak shear stress in the initial direction is higher than that in the opposite direction. The variation may be related to the anisotropic sand position caused by initial shear. The stress-displacement hysteresis loops present a tendency toward stabilization at the end of test. Among the sand-geotextile interfaces results, the *C*1-geotextile interface has the greatest shear stress and *C*3-geotextile interface has the least. The maximum peak shear stress of *C*1-geotextile, *C*2-geotextile, and *C*3-geotextile are 31.67, 30.83, and 28.33 kPa. It shows that fine particle-size gradation has an important effect on interparticle locking and shear strength. This observation is consistent with Wang et al. [21].

The interface vertical displacement versus shear displacement curves from the CDS test results for the three interfaces are shown in Figure 4. For all three particle-size gradations, vertical contraction is observed over the entire shearing process. During the shearing process, the change in vertical displacement is observed as volume change of the contact surface. In this study, compression of volume deformation of the contact surface is negative, and expansion is positive. The sand volume decreases throughout the entire process of cyclic shear. In initial cycle number, *C*2-geotextile interface contraction increases more rapidly than other sand-geotextile interfaces. The variation of vertical displacement with increasing cycle number for the three interfaces is shown in Figure 5. The interface vertical displacement generally increases with increasing number of cycles. However, the volumetric contraction of sand develops quickly at initial cycle number, and the increment gradually decreases with the increasing number of cycles for the three kinds of sand-geotextile interfaces. The curves between adjacent stress loops become closer to each other. This phenomenon is also observed by Liu et al. and Wang et al. [2, 16]. Of the three particle-size gradations, vertical displacement is minimum for discontinuously graded coarse *C*3-geotextile interface. The *C*2-geotextile interface has the largest vertical displacement, owing to the larger void ratio of sand. In the case of the well-graded sands, the smaller particles facilitate rolling and sliding of the larger particles, changing the kinematics of the shearing process.

4. Influence of Cyclic Shear History on Interface Shear Behaviour

Figure 6 shows the shear stress versus shear displacement curves obtained in the MDS and PCDS tests for the three interfaces under normal stress of 90 kPa. The tendency of the shear stress versus shear displacement curves is

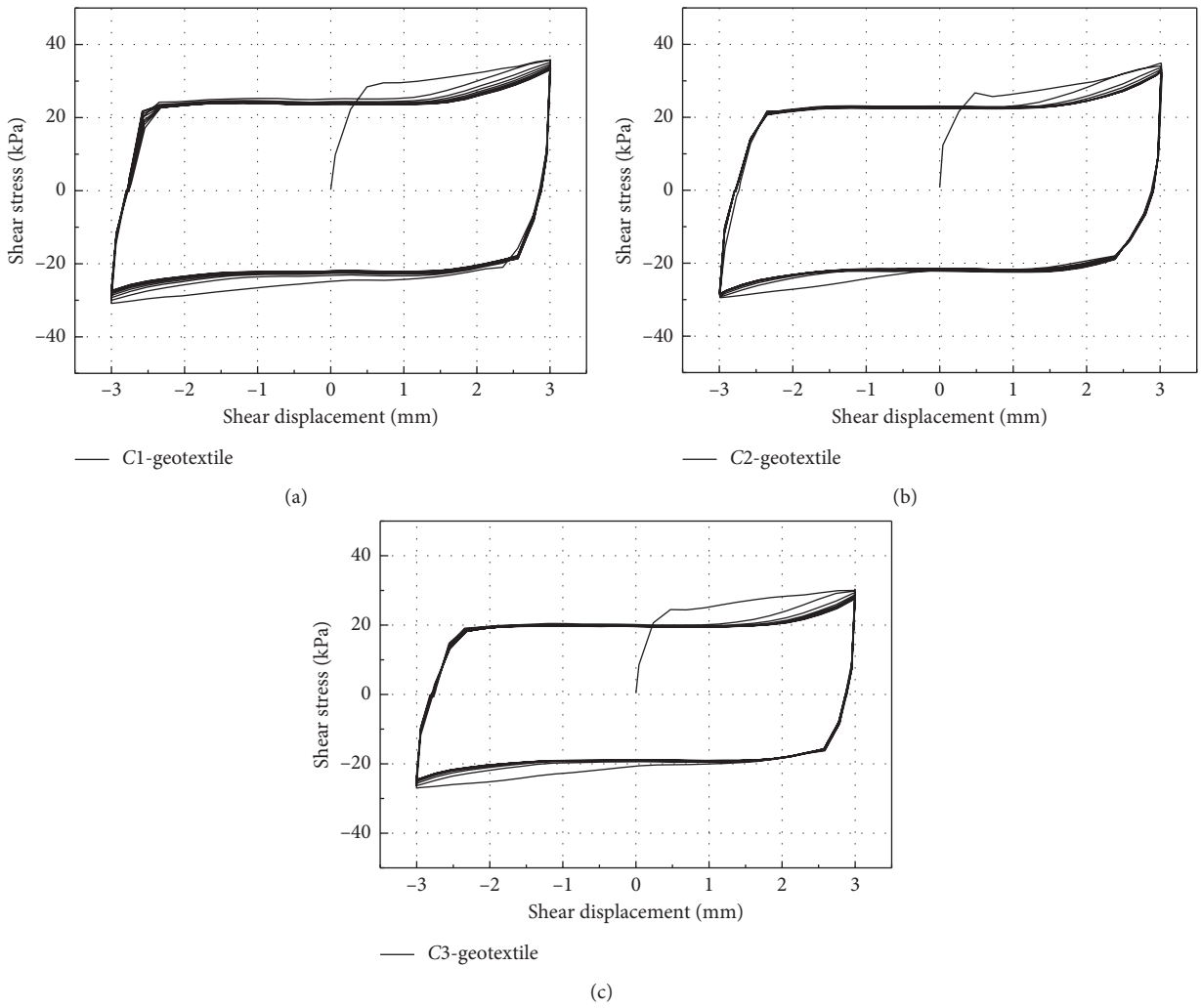

Figure 3: Effect of sand particle-size gradation on the interface shear stress-shear displacement curves in the CDS tests.

similar for the three coarse-grained sand-geotextile interfaces. No peak values are apparent, and all of these curves show shear hardening behaviour. In addition, in both the MDS tests and PCDS tests, the *C*1-geotextile interface has the greatest shear strength and the *C*3-geotextile interface has the least. It indicates that well-graded coarse sand has large interlocking of *C*1-geotextile interface. After the samples undergoing cyclic direct shear tests, the increment in interface shear strength is evident, especially for the *C*1-geotextile interface.

Figure 7 shows the interface vertical displacement versus shear displacement curves obtained from the MDS and PCDS tests for the three interfaces under normal stress of 90 kPa. Similar contraction tendency occurs during the entire process of volume development for all three interfaces. Particle-size gradation has greater influence on interface deformation in the PCDS tests compared with the CDS tests. The vertical displacement in the MDS tests is larger than that in the PCDS tests. A main factor for this phenomenon is that the interface densification is accelerated during the cyclic shearing. The influence of coarse-grained sand particle gradation on the interfacial deformation in the PCDS tests is greater than that in the MDS tests. This observation can be attributed to the difference of content of particle size. Comparing the vertical displacement of MDS with PCDS tests, the vertical displacement of *C*1-geotextile and *C*2-geotextile interface shows large difference. This results indicate that discontinuously graded coarse sand has more content of smaller particle size, which makes it more easily for rearrangement and crushing of particles [22].

Figure 8 shows the interface shear stress versus shear displacement curves obtained from the CDS and PCDS tests for the three interfaces under normal stresses of 30 kPa and 90 kPa. In the PCDS tests, the shear strength of the *C*1-geotextile interface and the *C*2-geotextile interface increases, whereas the shear strength of the *C*3-geotextile interface decreases. This phenomenon is more apparent under the lower normal stress. Under both levels of normal stress, *C*1-geotextile interface presents the greatest shear strength, whereas *C*3-geotextile interface presents the least shear strength. These results indicate that the well-graded coarse-grained sand has higher shear strength

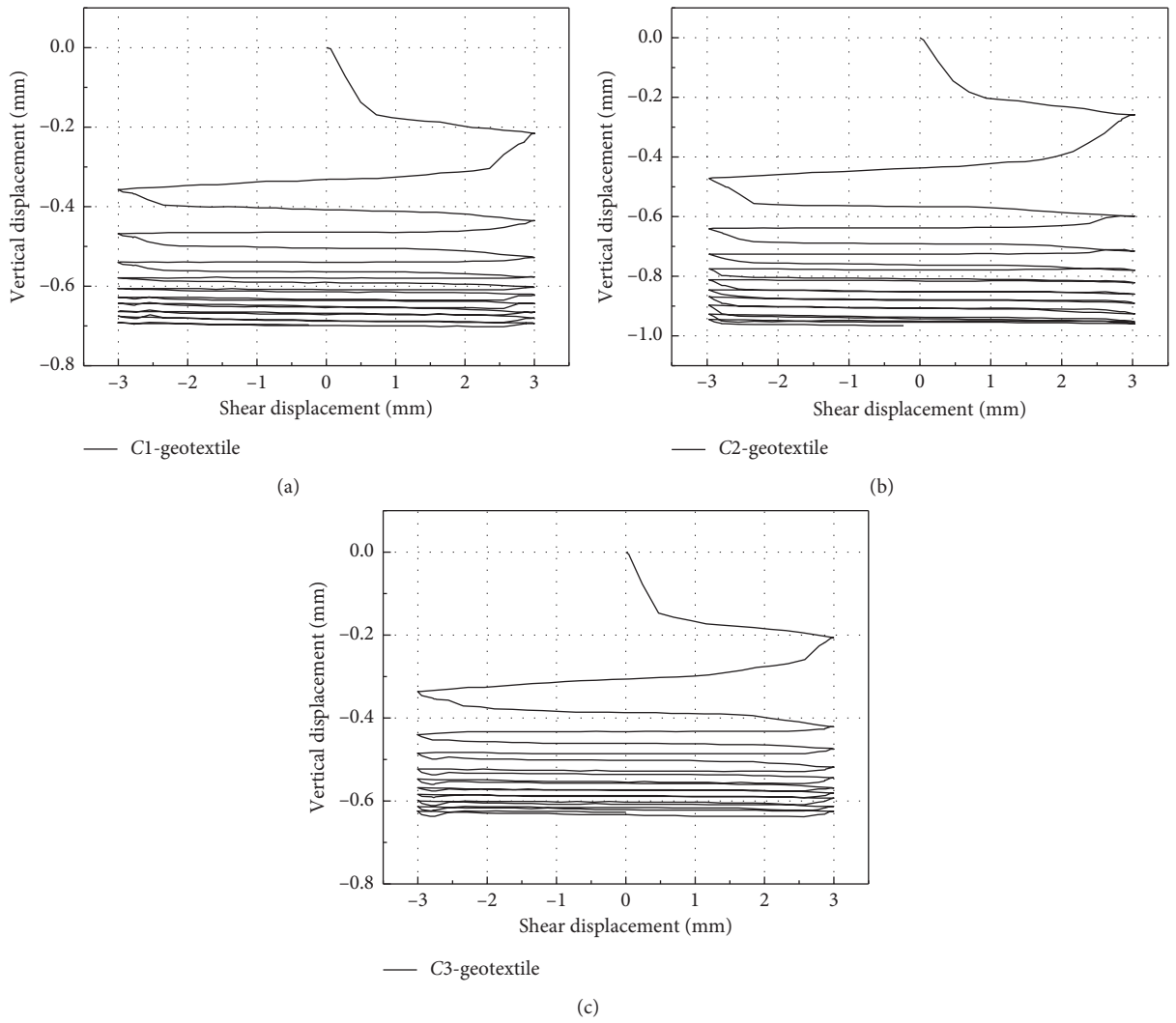

Figure 4: Effect of sand particle-size gradation on the interface vertical displacement-shear displacement curves in the CDS tests.

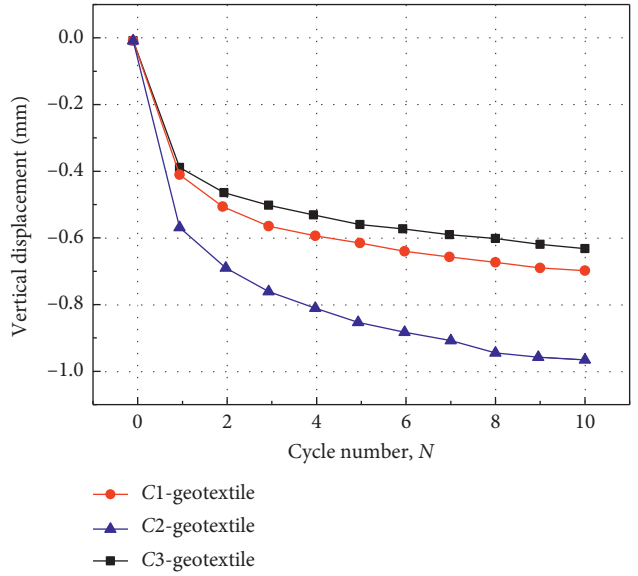

Figure 5: Relationships between interface vertical displacement and number of cycles with different sand particle-size gradations.

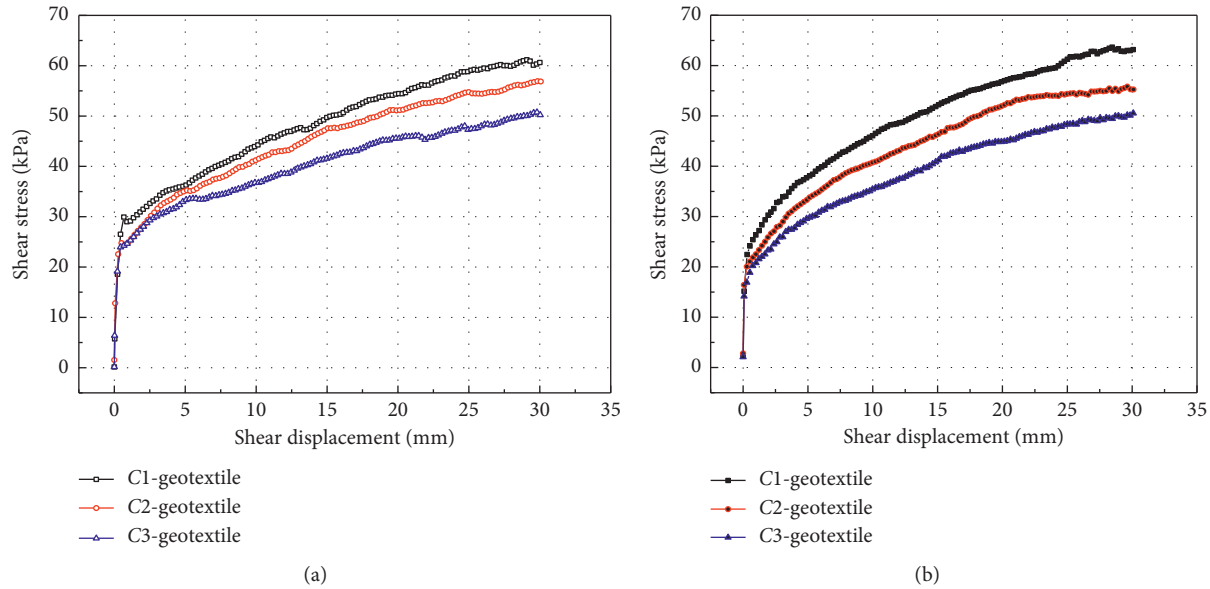

Figure 6: Effect of sand particle size on the interface shear stress-shear displacement curves in the (a) MDS and (b) PCDS tests.

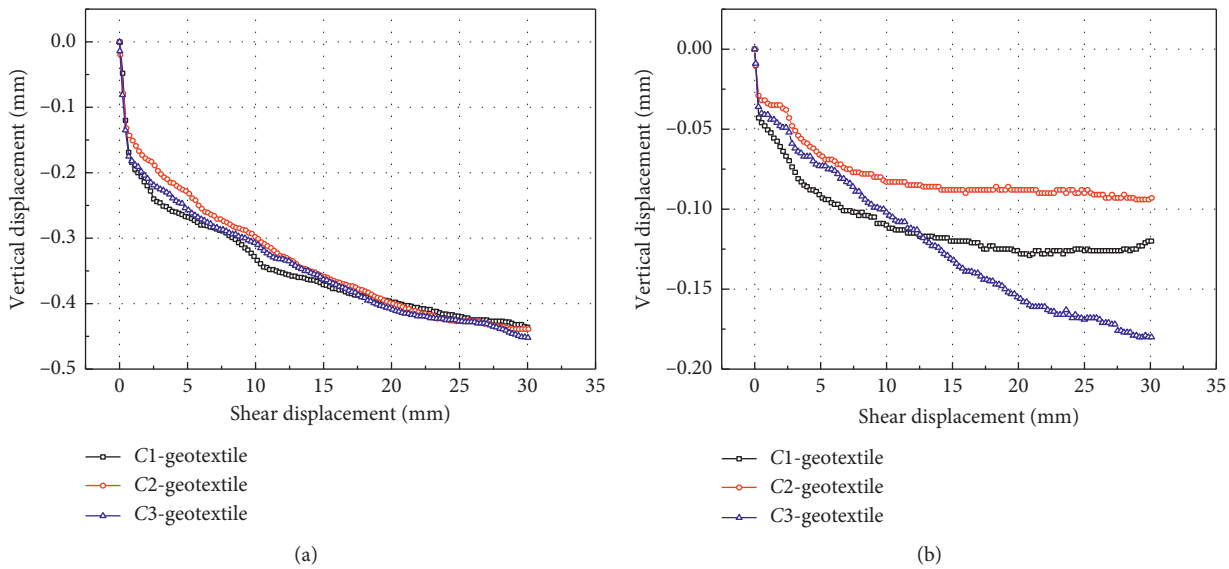

Figure 7: Effect of sand particle size on the interface vertical displacement-shear displacement curves in the (a) MDS and (b) PCDS tests.

and that sand particle-size gradation affects the shear strength of interfaces in MDS and PCDS tests.

Comparison of the vertical displacement versus shear displacement curves from the MDS and PCDS tests for the three interfaces under normal stresses of 30 kPa and 90 kPa is shown in Figure 9. The vertical displacement versus shear displacement curves for the three interfaces present greater differences, and the curve inflections change after the samples undergoning cyclic direct shear. Compared with the MDS tests, the PCDS tests result in more severe dilatation of the interfaces. This phenomenon can be attributed to the findings that densification of the interface is accelerated by cyclic direct shear. The rearrangement behaviour of sand particles consists mainly of scrolling and climbing, which mainly leads to more dilatation [23]. Under the normal stress of 30 kPa, the geotextile-reinforced sand undergoes vertical contraction during the initial stage and then exhibit dilatancy, whereas vertical contraction is observed throughout the entire course of shearing under the normal stress of 90 kPa. From comparison of Figure 8 with Figure 9, it is evident that the reinforced sand interfaces exhibit dilatancy associated with a corresponding decrease in shear stress under the normal stress of 30 kPa. In contrast, higher shear strength is observed for all three interfaces under the normal stress of 90 kPa.

5. Discussion

5.1. Shear Stiffness and Damping Ratios. Under cyclic loading of earthquakes and waves, the secant shear modulus and damping ratio of soil are two indispensable dynamic

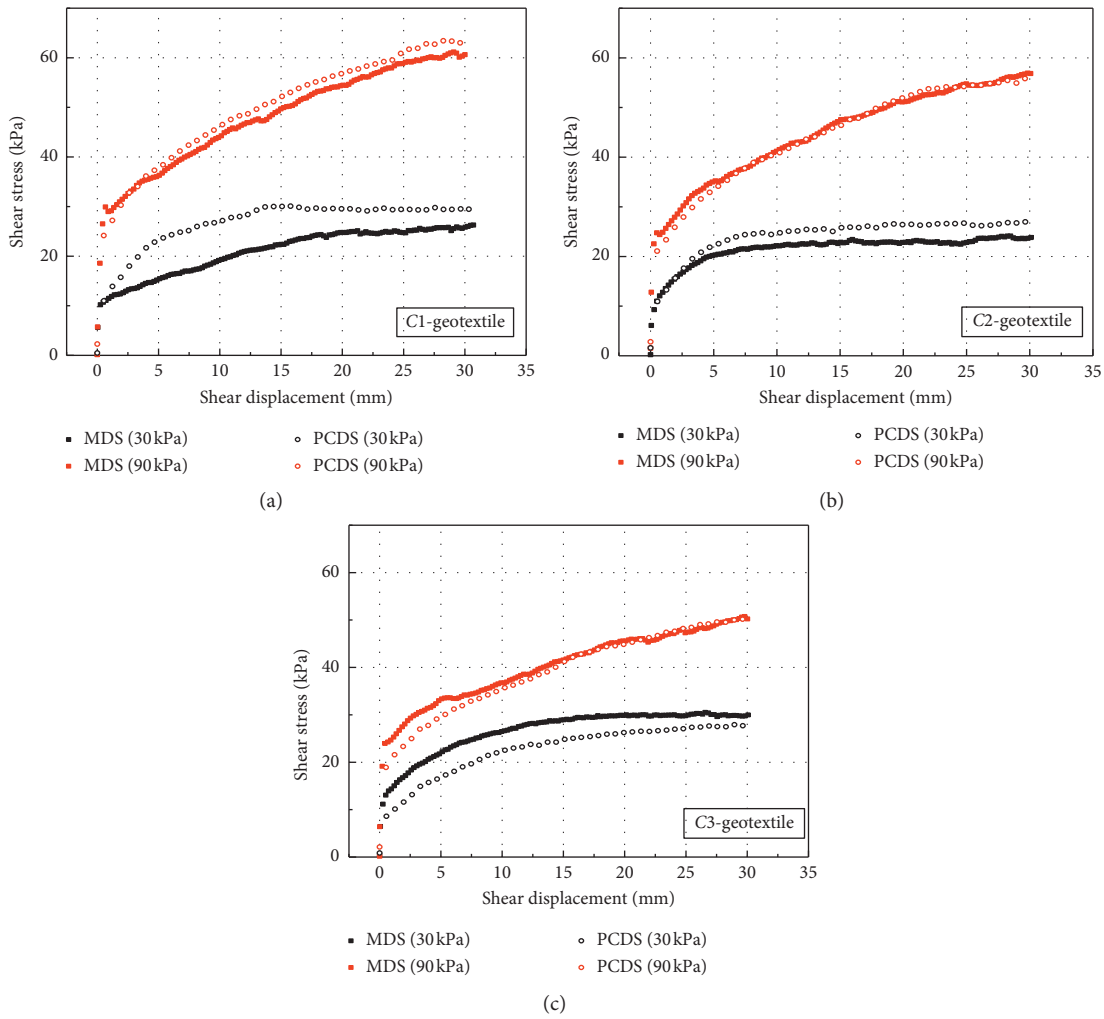

Figure 8: Comparison of the shear stress-shear displacement curves for the MDS and PCDS tests.

parameters, as typically used in equivalent linear ground motion analysis [24, 25]. Based on the definitions of shear stiffness and the damping ratio and the asymmetry of the same hysteresis loop in two shear directions, the shear stiffness (K) from a hysteresis loop are calculated according to the following formula:

$$K = \frac{\tau_{max} + \tau_{min}}{2\Delta a}, \quad (1)$$

where τ_{max} and τ_{min} are the maximum shear stress and the minimum shear stress for two shearing directions and Δa is the displacement semiamplitude. The damping ratio (D) is defined as

$$D = \frac{\Delta W}{2\pi\left(\left(\tau_{max}^2/2K\right) + \left(\tau_{min}^2/2K\right)\right)} = \frac{K\Delta W}{\pi\left(\tau_{max}^2 + \tau_{min}^2\right)}, \quad (2)$$

where ΔW is the total area enclosed by the loop. Figure 10 depicts the parameter definitions of shear stiffness and the damping ratio from the hysteresis loop.

Figure 11 shows the variations of the shear stiffness and damping ratio with increasing number of cycles for the three interfaces under normal stress of 90 kPa. The development of shear stiffness follows a similar pattern for all three interfaces. In the initial stage, interface shear stiffness decreases rapidly, and then the value of shear stiffness gradually tends to be stable at the end of cycle. This indicates that the interface responds to shear softening. However, the values of shear stiffness vary between the three interfaces for the same cycle number. Overall, the shear stiffness values for the *C*1-geotextile and *C*2-geotextile interfaces are higher than those for the *C*3-geotextile interface. It shows that well-graded sand in *C*1-geotextile has stronger resistance to sand deformation. Discontinuously graded coarse sand with weak internal contact force in *C*3-geotextile interface leads to lower shear resistance. As shown in Figure 11(b), there is a consistent pattern in the development of the damping ratios of all three interfaces. The damping ratio of each interface decreases rapidly with increasing number of cycles during the initial stage and then generally increases. This trend indicates that

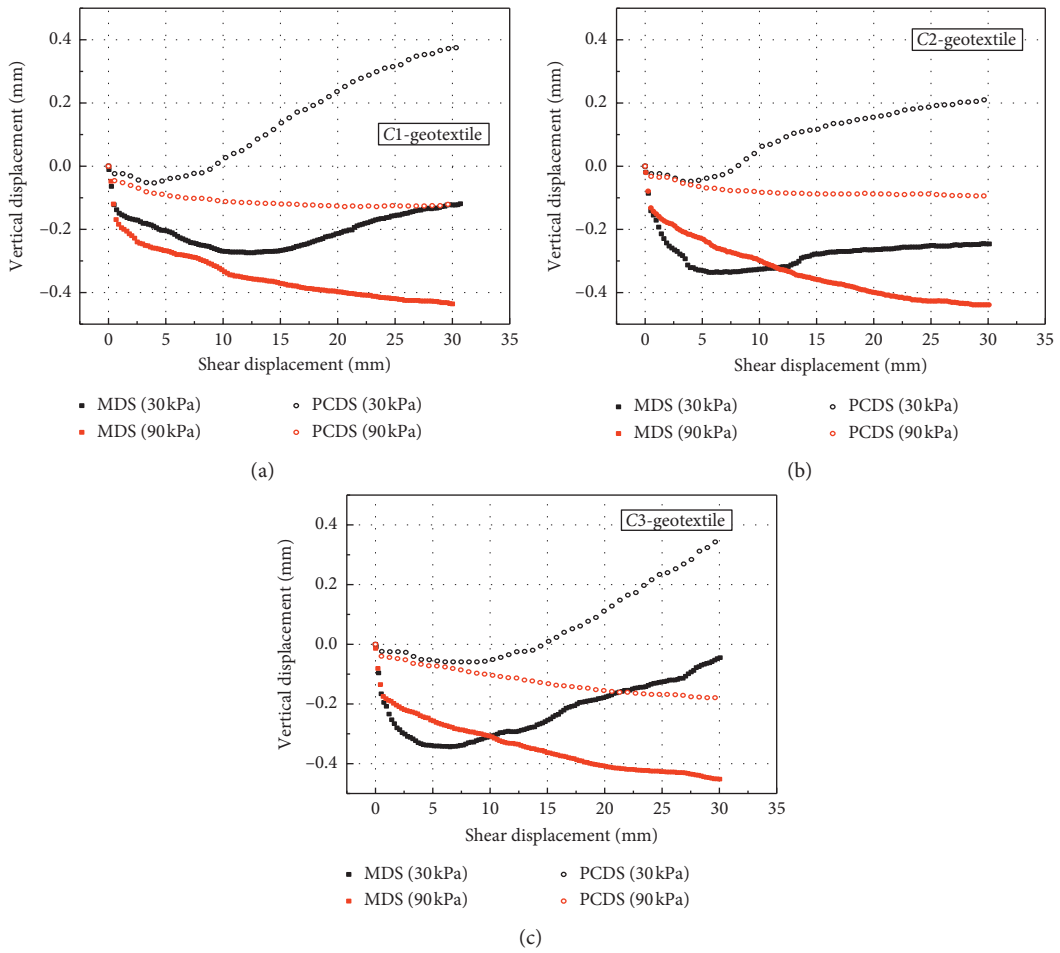

Figure 9: Comparison of the shear displacement-vertical displacement curves for the MDS and PCDS tests.

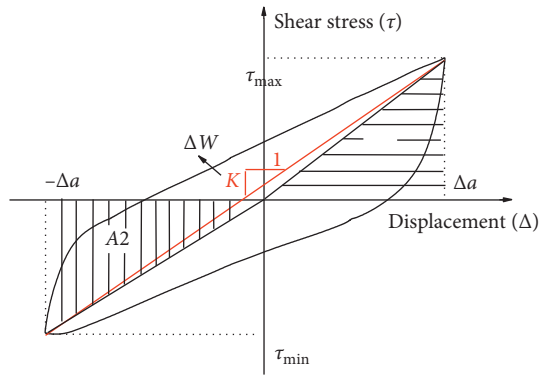

Figure 10: Calculation of the secant shear stiffness and damping ratio from a hysteresis loop.

the number of cycles affects the security and stability of the interface subjected to cyclic shear. In addition, the damping ratio of the well-graded sand-geotextile interface is larger than that of the other interfaces for the same cycle number. The results indicate that energy dissipates more slowly at a well-graded sand-geotextile interface subjected to cyclic shear.

5.2. Shear Strength Envelope Curve. Figure 12 shows the results of linear fitting between the shear strength of the three coarse sand-geotextile interfaces and the normal stress of these interfaces in the MDS and PCDS tests. These results indicate that in the range of vertical stress evaluated in this study, there is a strong linear relationship between interface shear strength and vertical stress. Therefore, the

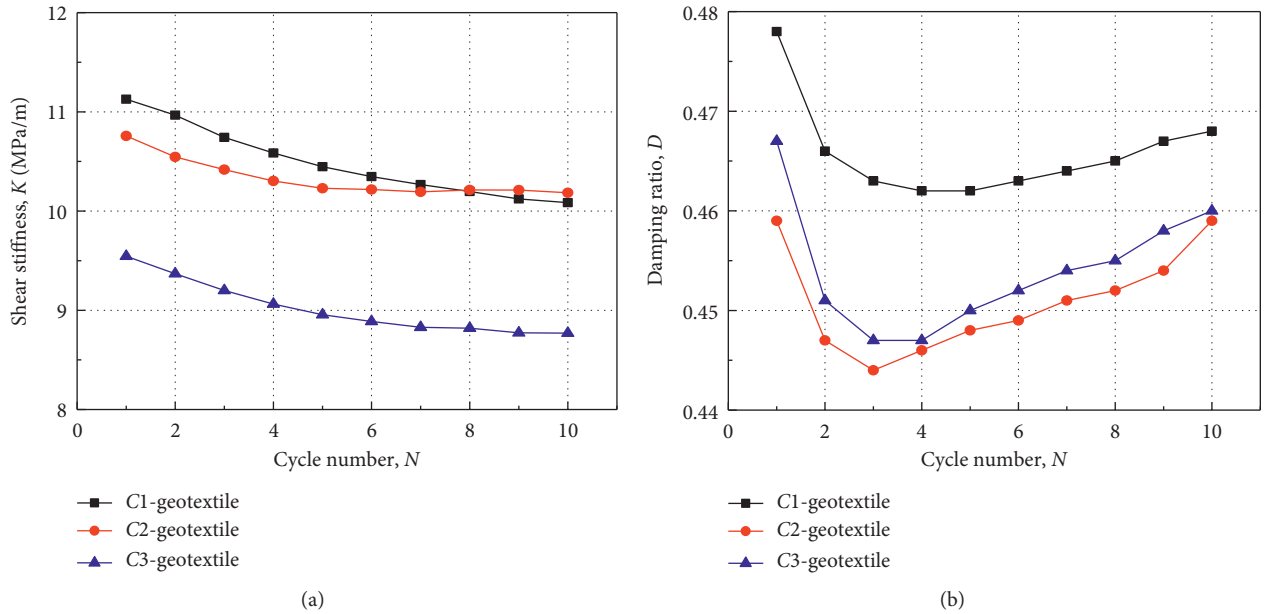

Figure 11: (a) Development of shear stiffness with cycle number and (b) development of damping ratio with cycle number.

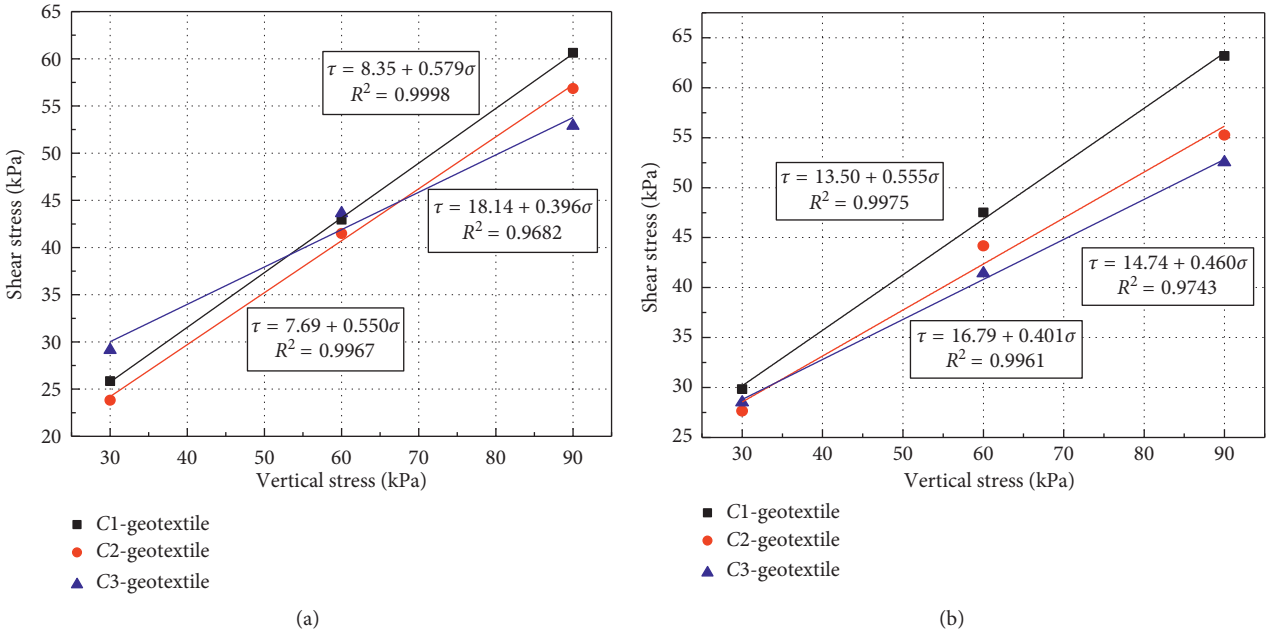

Figure 12: Shear strength envelopes for the (a) MDS and (b) PCDS tests.

Mohr–Coulomb criterion can be applied to express interface shear strength: $\tau = c + \sigma \tan \phi$, where c is the interface apparent adhesion; ϕ is the interface friction angle; and R^2 is the correlation parameter of the envelope curves. In the MDS tests, for the $C1$-geotextile, $C2$-geotextile, and $C3$-geotextile interfaces, the apparent adhesion (c) are 8.35, 7.69, and 18.14 kPa, respectively, and the friction angles (ϕ) are 30.1°, 28.8°, and 21.6°, respectively. It indicates that well-graded sand leads to an increase in the interface apparent adhesion and friction angle. In the PCDS tests, for the $C1$-geotextile interface, the apparent adhesion c increases from 8.35 kPa to 13.5 kPa, which is 61.7% higher than that in the MDS tests, and the friction angle ϕ is 29.1°. For the $C2$-geotextile interface, the apparent adhesion c increases from 7.69 kPa to 14.74 kPa, which is 91.7% higher than that in the MDS tests, and the friction angle ϕ decreases to 24.7°. For the $C3$-geotextile interface, the apparent adhesion c is 16.79 kPa and the friction angle ϕ is 21.8°. From the results of PCDS

test, the apparent adhesion of the interface increases, but the friction angle of the interface decreases.

6. Conclusions

The effect of particle-size gradation on shear strength and deformation of sand-geotextile interface was studied. Shear strength softening and shear contraction were observed in cyclic shearing for all three of the sand-geotextile interfaces. The interface with well-graded coarse sands had greater shear strength than the others. The interface with discontinuously graded coarse sands had the smallest value of contraction.

In the MDS and PCDS tests, shear hardening was observed at the sand-geotextile interfaces. Under lower normal stress, the geotextile-reinforced sands underwent vertical contraction during the initial stage and then exhibited dilatancy, whereas vertical contraction was observed throughout the entire shearing process under higher normal stress.

For all three sand particle-size distributions, the interface shear stiffness decreased with increasing number of cycles. The damping ratio decreased with increasing number of cycles during the initial shear cycles and then generally increased. Of the three interfaces at the same number of cycles, the one with well-graded coarse sands had the greatest shear stiffness and damping ratio.

The shear strength and apparent adhesion of the interfaces with well-graded and poorly graded coarse sands increased after cyclic direct shear was applied, whereas the interface with discontinuously graded coarse sands exhibited opposite tendencies.

Data Availability

The data used to support the findings of this study are available from the corresponding author upon request.

Conflicts of Interest

The authors declare that they have no conflicts of interest regarding the publication of this paper.

Acknowledgments

This study was supported by the National Key R&D Program of China (grant no. 2016YFC0800200), the National Natural Science Foundation of China (grant nos. 51678352, 51622810, 51978534, and 51878402), the Zhejiang Province Natural Foundation Projects of China (grant no. LR18E080001), and the Key Research and Development Program of Zhejiang Province (grant no. 2018C03038).

References

[1] H. Vidal, *The Principal of Reinforced Earth*, Highway Research Record, Washington, DC, USA, 1969.

[2] F.-Y. Liu, P. Wang, X. Geng, J. Wang, and X. Lin, "Cyclic and post-cyclic behaviour from sand-geogrid interface large-scale direct shear tests," *Geosynthetics International*, vol. 23, no. 2, pp. 129–139, 2016.

[3] G. Gao and M. A. Meguid, "Effect of particle shape on the response of geogrid-reinforced systems: insights from 3D discrete element analysis," *Geotextiles and Geomembranes*, vol. 46, no. 6, pp. 685–698, 2018.

[4] E. Guler, M. Hamderi, and M. M. Demirkan, "Numerical analysis of reinforced soil-retaining wall structures with cohesive and granular backfills," *Geosynthetics International*, vol. 14, no. 6, pp. 330–345, 2007.

[5] M. Abdesssemed, S. Kenai, and A. Bali, "Experimental and numerical analysis of the behavior of an airport pavement reinforced by geogrids," *Construction and Building Materials*, vol. 94, pp. 547–554, 2015.

[6] Z. Wang, F. Jacobs, and M. Ziegler, "Visualization of load transfer behaviour between geogrid and sand using PFC2D," *Geotextiles and Geomembranes*, vol. 42, no. 2, pp. 83–90, 2014.

[7] Z. Wang, F. Jacobs, and M. Ziegler, "Experimental and DEM investigation of geogrid-soil interaction under pullout loads," *Geotextiles and Geomembranes*, vol. 44, no. 3, pp. 230–246, 2016.

[8] R. A. Jewell and C. P. Wroth, "Direct shear tests on reinforced sand," *Géotechnique*, vol. 37, no. 1, pp. 53–68, 1987.

[9] S. A. Tan, S. H. Chew, and W. K. Wong, "Sand-geotextile interface shear strength by torsional ring shear tests," *Geotextiles and Geomembranes*, vol. 16, no. 3, pp. 161–174, 1998.

[10] L. Carbone, J. P. Gourc, P. Carrubba, P. Pavanello, and N. Moraci, "Dry friction behaviour of a geosynthetic interface using inclined plane and shaking table tests," *Geotextiles and Geomembranes*, vol. 43, no. 4, pp. 293–306, 2015.

[11] A. Mirzaalimohammadi, M. Ghazavi, M. Roustaei, and S. H. Lajevardi, "Pullout response of strengthened geosynthetic interacting with fine sand," *Geotextiles and Geomembranes*, vol. 47, no. 4, pp. 530–541, 2019.

[12] A. Afzali-Nejad, A. Lashkari, and P. T. Shourijeh, "Influence of particle shape on the shear strength and dilation of sand-woven geotextile interfaces," *Geotextiles and Geomembranes*, vol. 45, no. 1, pp. 54–66, 2017.

[13] D. J. U. Infante, G. M. A. Martinez, P. A. Arrua, and M. Eberhardt, "Shear strength behavior of different geosynthetic reinforced sand structure from direct shear test," *International Journal of Geosynthetics and Ground Engineering*, vol. 2, no. 2, pp. 1–16, 2016.

[14] F. B. Ferreira, C. S. Vieira, and M. L. Lopes, "Direct shear behaviour of residual soil-geosynthetic interfaces-influence of soil moisture content, soil density and geosynthetic type," *Geosynthetics International*, vol. 22, no. 3, pp. 257–272, 2015.

[15] Anubhav and P. K. Basudhar, "Interface behavior of woven geotextile with rounded and angular particle sand," *Journal of Materials In Civil Engineering*, vol. 25, no. 12, pp. 1970–1974, 2013.

[16] J. Wang, F. Y. Liu, P. Wang, and Y. Q. Cai, "Particle size effects on coarse soil-geogrid interface response in cyclic and post-cyclic direct shear tests," *Geotextiles and Geomembranes*, vol. 44, no. 6, pp. 854–861, 2016.

[17] R. Alaie and R. J. Chenari, "Cyclic and post-cyclic shear behaviour of interface between geogrid and EPS beads-sand backfill," *KSCE Journal of Civil Engineering*, vol. 22, no. 9, pp. 3340–3357, 2018.

[18] ASTM D5321, *Standard Test Method for Determining the Ceofficient of Soil and Geosynthetic or Geosynthetic and Geosynthetic Friction by the Direct Shear Method*, ASTM International, West Conshohocken, PA, USA, 2002.

[19] M. L. Lopes and R. Silvano, "Soil/geotextile interface behaviour in direct shear and pullout movements," *Geotechnical and Geological Engineering*, vol. 28, no. 6, pp. 791–804, 2010.

[20] G. Zhang and J.-M. Zhang, "Experimental study on behavior of interface between sand and geotextile," *Rock and Sand Mechanics*, vol. 27, no. 1, pp. 51–55, 2006.

[21] J.-J. Wang, H.-P. Zhang, S.-C. Tang, and Y. Liang, "Effects of particle size distribution on shear strength of accumulation soil," *Journal of Geotechnical and Geoenvironmental Engineering*, vol. 139, no. 11, pp. 1994–1997, 2013.

[22] Y. Xu, D. J. Williams, M. Serati et al., "Effects of scalping on direct shear strength of crusher run and crusher run/geogrid interface," *Journal of Materials in Civil Engineering*, vol. 30, no. 9, Article ID 04018206, 2018.

[23] H.-L. Wang, W.-H. Zhou, Z.-Y. Yin et al., "Effect of grain size distribution of sandy soil on shearing behaviors at soil–structure interface," *Journal of Materials in Civil Engineering*, vol. 31, no. 10, Article ID 04019238, 2019.

[24] C. J. Nye and P. J. Fox, "Dynamic shear behavior of a needle-punched geosynthetic clay liner," *Journal of Geotechnical and Geoenvironmental Engineering*, vol. 133, no. 8, pp. 973–983, 2007.

[25] C. S. Vieira, M. L. Lopes, and L. M. Caldeira, "Sand-geotextile interface characterisation through monotonic and cyclic direct shear tests," *Geosynthetics International*, vol. 20, no. 1, pp. 26–38, 2013.